Supporting Information

Solution Processible Triphenylphosphine-Oxide-Cored Dendritic Hosts Featuring Thermally Activated Delayed Fluorescence for Power-Efficient Blue Electrophosphorescent Devices

Mingming Zhang,[a,b] Liang Chen,[a,b] Xiushang Xu,[a] Shumeng Wang,[a] Junqiao Ding,*[,a,b] Lixiang Wang*[,a,b]

[a] *State Key Laboratory of Polymer Physics and Chemistry, Changchun Institute of Applied Chemistry, Chinese Academy of Sciences, Changchun 130022, P. R. China*

[b] *University of Science and Technology of China, Hefei 230026, P. R. China*

Table of Contents:

Experimental section

General information: The Bruker Avance 400 NMR spectrometer was used to measure ^{1}H, ^{13}C and ^{31}P NMR spectra. AXIMA CFR MS apparatus was used to record MALDI/TOF mass spectra. Elemental analysis was recorded with a Bio-Rad elemental analysis system. Perkin-Elmer-TGA 7 and Perkin-Elmer-DSC 7 apparatus were used to analyze thermal gravimetric analysis (TGA) and differential scanning calorimetry (DSC) under nitrogen at a heating rate of 10 ^{o}C min^{-1}, respectively. PL spectra and UV-vis absorption were recorded using a Perkin-Elmer LS 50B spectrofluorometer and a Perkin-Elmer Lambda 35 UV-vis spectrometer, respectively. Phosphorescent spectra were measured in film at 77 K. The film PLQY was measured with an Binson C9920-2 integrating sphere under N_2. The fluorescence lifetimes were analyzed with FLS920 Edinburgh fluorescence spectrometer under nitrogen and excited at 375 nm. Cyclic voltammetry characteristics was recorded in dichloromethane with a conventional three-electrode system with Fc/Fc^{+} couple as reference and the supporting electrolyte was 0.1 mol/L n-Bu_4NClO_4. The HOMO and LUMO levels were calculated according to the equation HOMO = -e(E_{ox}^{onset} + 4.8 V), LUMO = HOMO + E_g, where E_{ox}^{onset} is the onset value of the first oxidation wave and the E_g is the optical bandgap estimated from the absorption onset.

Device fabrication and testing: Firstly, the ITO-glass substrates (20 Ω per square) was cleaned and perform UVO treatment and then a 40 nm-thick PEDOT:PSS film was spin-coated on the ITO-glass substrates. After drying at 120 ^{o}C for 30 min, the substrates were transferred to glove box filled N_2. The emitting layer material was

dissolved in chlorobenzene and spin-coated on the PEDOT:PSS layer and then annealed at 100 ^{o}C for 40 minutes. Subsequently, the substrate was transferred to vacuum evaporation chamber to sequentially evaporate and deposited a 5 nm-thick film of TSPO1, 45 nm-thick film of TmPyPB, 1 nm-thick film of LiF and 100 nm-thick film of Al on top of the emitting layer via a shadow mask and evaporation operation was carried out at a base pressure less than 10^{-6} Torr (1 Torr = 133.32 Pa). The *J-V-L* plots were recorded using a Keithley 2400 and 2000 source measurement unit with a silicon photodiode as reference. The SpectraScan PR650 spectrophotometer was used to record the EL spectra. All the measurements were performed at room temperature under ambient conditions. EQE was calculated from the EL spectra, luminance, current density and with a Lambertian distribution assumption.

***Synthesis*:** Reagents and starting materials used in this work were purchased from commercial chemical company without further purification. Solvents (THF, toluene, DMF) for chemical synthesis were purified with Na_2SO_4 and then sodium. The dendrons oligocarbazole (CzCz), carbazole/acridine hybrid (AcCz), oligoacridine (AcAc) and $Ir(mpim)_3$ were prepared according to literatures.[1-3]

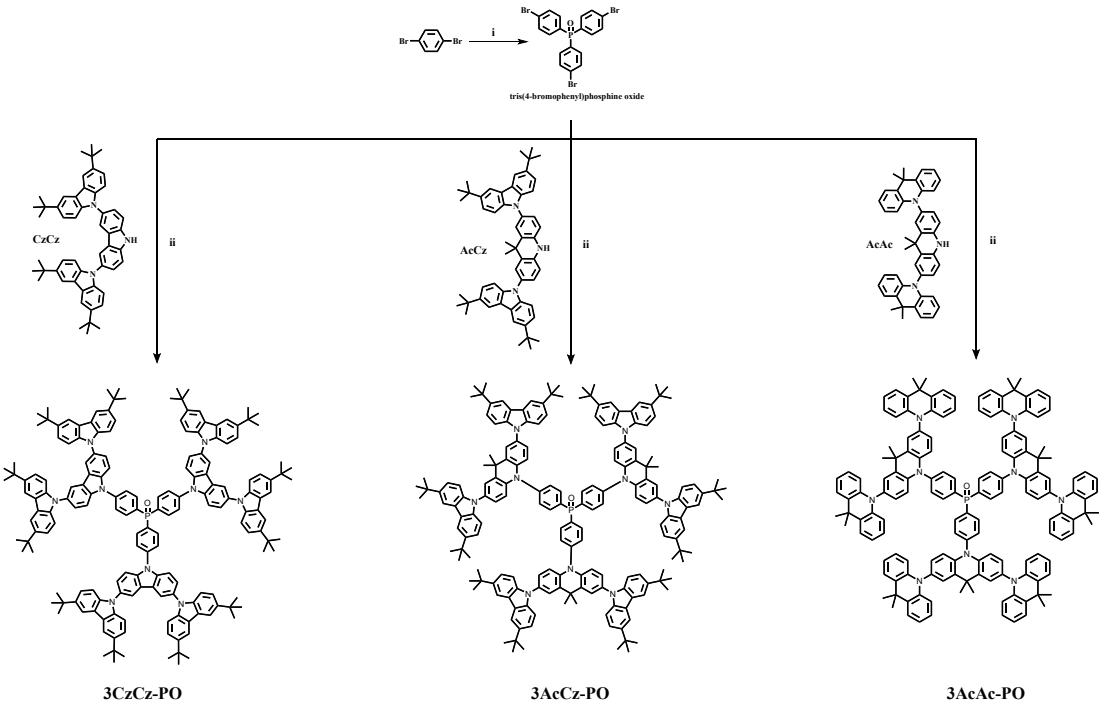

Scheme S1. Synthetic route of the dendrimer 3CzCz-PO, 3AcCz-PO and 3AcAc-PO. Reagents and conditions: (i) Mg, I_2, $POCl_3$, THF, 0 ^oC ; (ii) $Pd_2(dba)_3$, $HP(t\text{-}Bu_3).BF_4$, t-BuONa, toluene, 100 ^oC.

tris(4-bromophenyl)phosphine oxide: Under dry N_2 atmosphere, a little iodine and magnesium (1 equiv.) were mixed within a flask and the 15 ml THF solution of 1,4-dibromobenzene (1 equiv.) was added slowly. Then the temperature of reaction system was set at 60 °C and the mixtures were stirred evenly to generate Grignard reagent until the magnesium disappear. After that, the temperature of reaction system was lowered to 0 °C. Added $POCl_3$ (0.3 equiv.) into the reaction system and stirred for another 3 h. After completion of the reaction, water was added to quench Grignard reagent, and CH_2Cl_2 was used for extraction of the system. Then, the organic phase would be isolated followed by removing the solvent. The column chromatography silica gel (eluent: CH_2Cl_2/ethyl acetate = 10:1) was applied to purify the residual solid after

distillation. Finally, desired white solid was obtained (430 mg, 44%). ^{1}H NMR (400 MHz, $CDCl_3$): δ = 7.63 (dd, *J* = 8.4, 2.3 Hz, 6H), 7.49 (dd, *J* = 11.7, 8.4 Hz, 6H).

*General Procedure for the Synthesis of **3CzCz-PO**, **3AcCz-PO** and **3AcAc-PO***: Tris(4-bromophenyl)phosphine oxide (1 equiv.), dendrimer segment (3.5 equiv.), $Pd_2(dba)_3$ (0.15 equiv.), HP(*t*-Bu)$_3$BF$_4$(0.8 equiv.), *t*-BuONa (6 equiv.) were added to degassed toluene under N_2. The reaction system was set at 105 ^{o}C and held for 18 h with continuous stir. When the reaction is complete, toluene was added into the system thus the reaction solution was diluted. Then reaction solution was washed with brine. Subsequently, the organic phase in the top layer was isolated and solvent was removed at elevated temperature by vacuum distillation. Finally, the residual solid was purified with silica gel column chromatography (eluent: petroleum ether: CH_2Cl_2 = 1:4) to give white solid.

3CzCz-PO (620 mg, 46%) ^{1}H NMR (400 MHz, C_6D_6): δ = 8.49 (s, 12H), 8.30 (dd, *J* = 11.3, 8.3 Hz, 6H), 7.99 (d, *J* = 1.8 Hz, 6H), 7.58 – 7.53 (m, 24H), 7.52 – 7.48 (m, 12H), 7.34 (d, *J* = 8.6 Hz, 6H), 1.45 (s, 108H). ^{13}C NMR (126 MHz, $CDCl_3$) δ = 142.73, 139.98, 139.60, 134.32, 134.23, 131.73, 127.12, 127.02, 126.22, 124.63, 123.62, 123.20, 119.50, 116.29, 111.07, 108.97, 34.73, 32.03. ^{31}P NMR (162 MHz, $CDCl_3$) δ = 26.77. MALDI-TOF (m/z): 2838.3 [M^+]. Anal. calcd. For $C_{174}H_{174}N_9OP$: C, 85.71; H, 7.19; N,5.17 Found: C, 85.72; H, 7.23; N, 5.31.

3AcCz-PO (670 mg, 53%) ^{1}H NMR (400 MHz, C_6D_6): δ = 8.43 (s, 12H), 8.26 (dd, *J* = 11.2, 8.2 Hz, 6H), 7.65 (d, *J* = 2.0 Hz, 6H), 7.53 – 7.47 (m, 24H), 7.32 (d, *J* = 6.8 Hz, 6H), 7.12 (d, *J* = 2.1 Hz, 6H), 6.49 (d, *J* = 8.7 Hz, 6H), 1.49 (s, 18H), 1.43 (s, 108H). ^{13}C NMR (126 MHz, $CDCl_3$) δ = 145.29, 142.59, 139.55, 139.08, 135.29, 135.21, 132.73, 131.74, 131.47, 125.19, 124.47, 123.54, 123.11, 116.26, 115.21, 109.02, 36.64, 34.71, 32.03. ^{31}P NMR (162 MHz, $CDCl_3$) δ = 28.46. MALDI-TOF (m/z): 2564.5 [M+]. Anal. calcd. For $C_{183}H_{192}N_9OP$: C, 85.71; H, 7.55; N,4.92; Found: C, 85.71; H, 7.53; N, 4.66.

3AcAc-PO (560 mg, 57%) ^{1}H NMR (400 MHz, C_6D_6): δ = 8.16 (dd, *J* = 11.3, 8.3 Hz, 6H), 7.39 (dd, *J* = 5.2, 1.9 Hz, 18H), 7.30 (d, *J* = 6.5 Hz, 6H), 6.96 – 6.88 (m, 24H), 6.85 (dd, *J* = 8.6, 2.2 Hz, 6H), 6.56 (dd, *J* = 7.7, 1.5 Hz, 12H), 6.48 (d, *J* = 8.6 Hz, 6H), 1.65 (s, 36H), 1.32 (s, 18H). ^{13}C NMR (126 MHz, C_6D_6) δ 145.30, 142.04, 140.35, 135.66, 135.54, 135.46, 134.54, 133.49, 132.37, 132.27, 130.54, 130.08, 128.91, 127.06, 126.05, 121.35, 116.75, 114.65, 36.87, 36.44, 31.83, 31.00. ^{31}P NMR (162 MHz, C_6D_6) δ = 22.80. MALDI-TOF (m/z): 2143.7 [M^+]. Anal. calcd. For $C_{153}H_{132}N_9OP$: C, 85.72; H, 6.21; N,5.88; Found: C, 85.72; H, 6.13; N, 5.45.

REFERENCES

1. D. Xia, B. Wang, B. Chen, S. Wang, B. Zhang, J. Ding, L. Wang, X. Jing and F. Wang, *Angew. Chem. Int. Ed.*, 2014, **53**, 1048-1052.
2. X. Wang, S. Wang, J. Lv, S. Shao, L. Wang, X. Jing and F. Wang, *Chem. Sci.*, 2019, **10**, 2915-2923.

3. M. Zhang, X. Li, S. Wang, J. Ding, L. Wang, *Org. Electron.* 2019, **68**, 193-199
4. C. Duan, J. Li, C. Han, D. Ding, H. Yang, Y. Wei, H. Xu, *Chem. Mater.* 2016, **28**, 5667−5679
5. J. Jin, Y. Tao, H. Jiang, R. Chen, G. Xie, Q. Xue, C. Tao, L. Jin, C. Zheng and W. Huang, *Adv. Sci.*, 2018, **5**, 1800292.
6. X. Jing, L. Jiang, K. Sun, W. Tian and W. Jiang, *New J. Chem.*, 2018, **42**, 4081-4088.
7. X. Ban, K. Sun, Y. Sun, B. Huang and W. Jiang, *ACS Appl. Mater. Interfaces*, 2016, **8**, 2010-2016.
8. X. Ban, K. Sun, Y. Sun, B. Huang, S. Ye, M. Yang and W. Jiang, *ACS Appl. Mater. Interfaces*, 2015, **7**, 25129-25138.
9. X. Wang, S. Wang, Z. Ma, J. Ding, L. Wang, X. Jing and F. Wang, *Adv. Funct. Mater.*, 2014, **24**, 3413-3421.
10. Y. Wang, S. Wang, J. Ding, L. Wang, X. Jing and F. Wang, *Chem. Commun.*, 2016, **53**, 180-183.
11. Y. Wang, S. Wang, S. Shao, J. Ding, L. Wang, X. Jing and F. Wang, *Dalton Trans.*, 2015, **44**, 1052-1059.
12. S. Wang, L. Zhao, B. Zhang, J. Ding, Z. Xie, L. Wang and W. Y. Wong, *iScience*, 2018, **6**, 128-137.
13. Y. Tao, X. Guo, L. Hao, R. Chen, H. Li, Y. Chen, X. Zhang, W. Lai and W. Huang, *Adv. Mater.*, 2015, **27**, 6939-6944.

Table S1. Calculation of TADF rate constants for the dendrimers in neat film.

	Φ_{PL}[a] [%]	Φ_{PF}/Φ_{DF}[b] [%]	τ_p[c] [ns]	τ_d[c] [μs]	k_{PF}[d] [$\times 10^6$ s^{-1}]	k_{DF}[d] [$\times 10^3$ s^{-1}]	k_{ISC}[d] [$\times 10^6$ s^{-1}]	k_{RISC}[d] [$\times 10^4$ s^{-1}]
3CzCz-PO	31	31/0	23	-	11.5	-	7.9	-
3AcCz-PO	22	16/6	31	1.5	5.2	4.0	1.4	5.6
3AcAc-PO	33	29/4	31	1.0	9.4	4.0	1.1	4.7

[a]Absolute PLQY measured in film with integrating sphere under N_2. [b]Estimated according to the prompt and delayed proportions in transient decay curve. [c]Lifetimes of prompt emission (τ_p) and delayed emission (τ_d) measured in film at 298 K in N_2. [d]Calculated according to the literature.[4]

Table S2. Summary of device performance based on 3AcAc-PO with different doping concentration of $Ir(mpim)_3$.

Concentration [wt.%]	V_{on} [a] [V]	L_{max} [cd m^{-2}]	CE [b] [cd A^{-1}]	PE [b] [lm W^{-1}]	EQE [b] [%]	CIE [c] [x, y]
5	4.0	20056	10.2	7.0	4.0	(0.21, 0.44)
10	3.4	21936	21.0	16.6	8.2	(0.21, 0.44)
15	3.0	22125	29.1	26.3	11.3	(0.21, 0.44)
20	2.6	25815	40.7	46.4	15.8	(0.21, 0.44)
25	2.6	24512	37.3	39.8	14.5	(0.22, 0.45)
30	2.4	22241	36.3	39.8	14.2	(0.22, 0.45)
35	2.4	21159	34.9	38.6	13.5	(0.22, 0.45)

[a]Turn-on voltage at a brightness of 1 cd m^{-2}; [b]Maximum values for current efficiency (CE), power efficiency (PE) and EQE, respectively; [c]CIE at 1000 cd m^{-2}.

Table S3. Device performance comparison for solution-processed blue PhOLEDs.

Ref.	V_{on} [a] [V]	PE [b] [lm W^{-1}]
This work	2.6	46.2
Ref. [1]	3.6	28.9
Ref. [5]	3.5	30.5
Ref. [6]	5.3	13.5
Ref. [7]	2.8	22.0
Ref. [8]	2.7	22.5
Ref. [9]	5.3	14.1
Ref. [10]	2.7	30.3
Ref. [11]	3.4	23.3
Ref. [12]	2.9	34.2
Ref. [13]	3.8	19.0

[a]Turn-on voltage at a brightness of 1 cd m^{-2}; [b]Maximum values for power efficiency (PE).

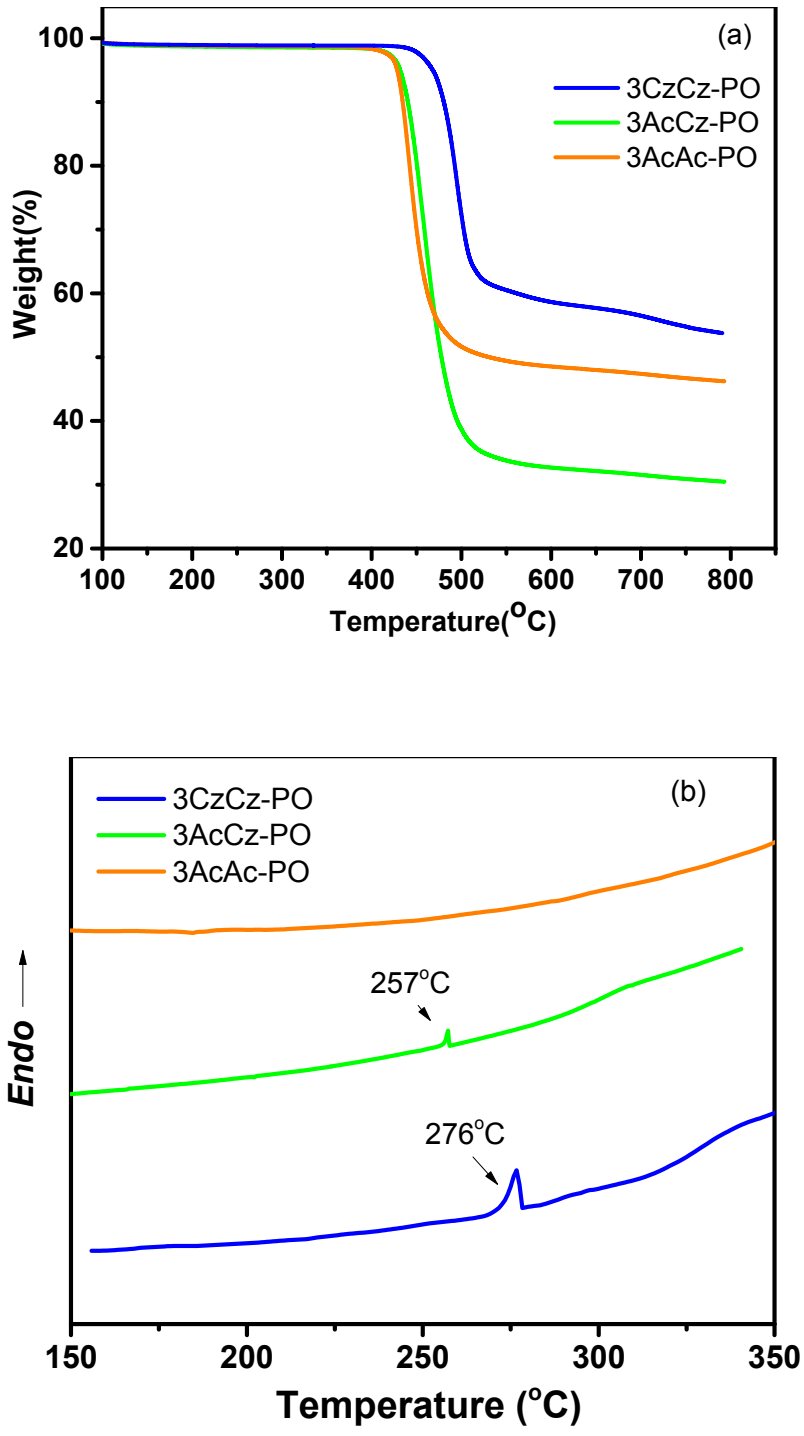

Figure S1. (a) TGA spectra for 3CzCz-PO, 3AcCz-PO and 3AcAc-PO, at a heating rate of 10 °C/min under N_2. (b) DSC spectra for 3CzCz-PO, 3AcCz-PO and 3AcAc-PO, at a heating rate of 10 °C/min under N_2.

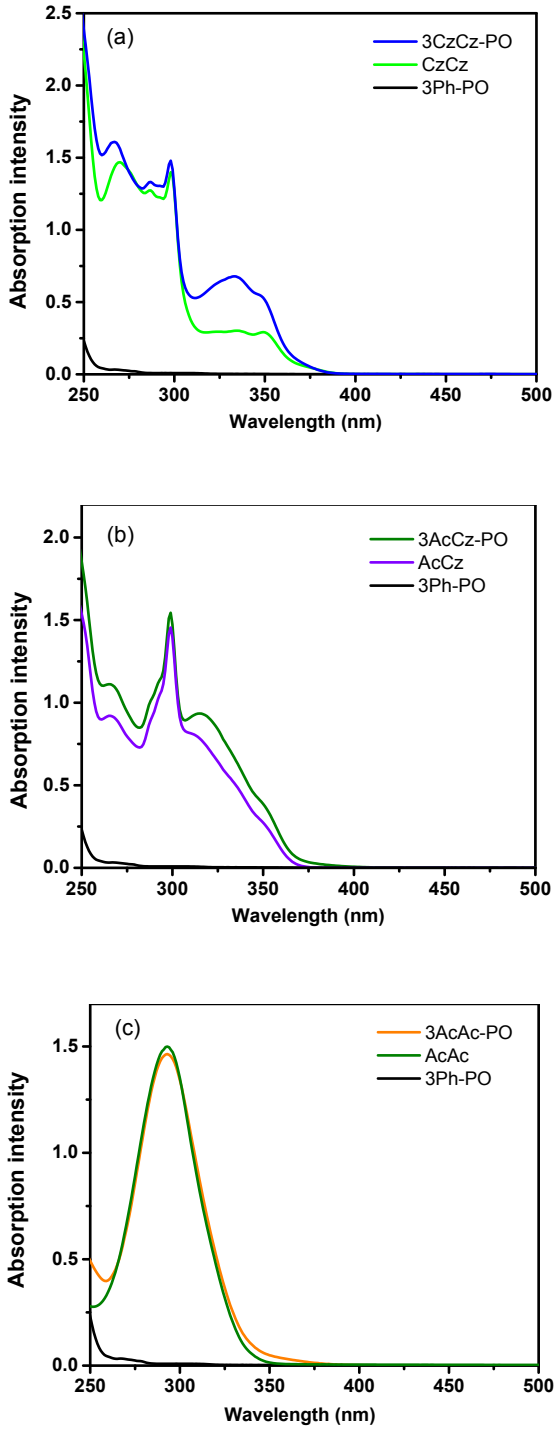

Figure S2. Absorption comparison of (a) 3CzCz-PO, (b) 3AcCz-PO and (c) 3AcAc-PO with corresponding donor and acceptor fragments in CH_2Cl_2 solution. (Concentration: 1×10^{-5} mol/L for dendrimers and 3Ph-PO and 3×10^{-5} mol/L for donor fragments)

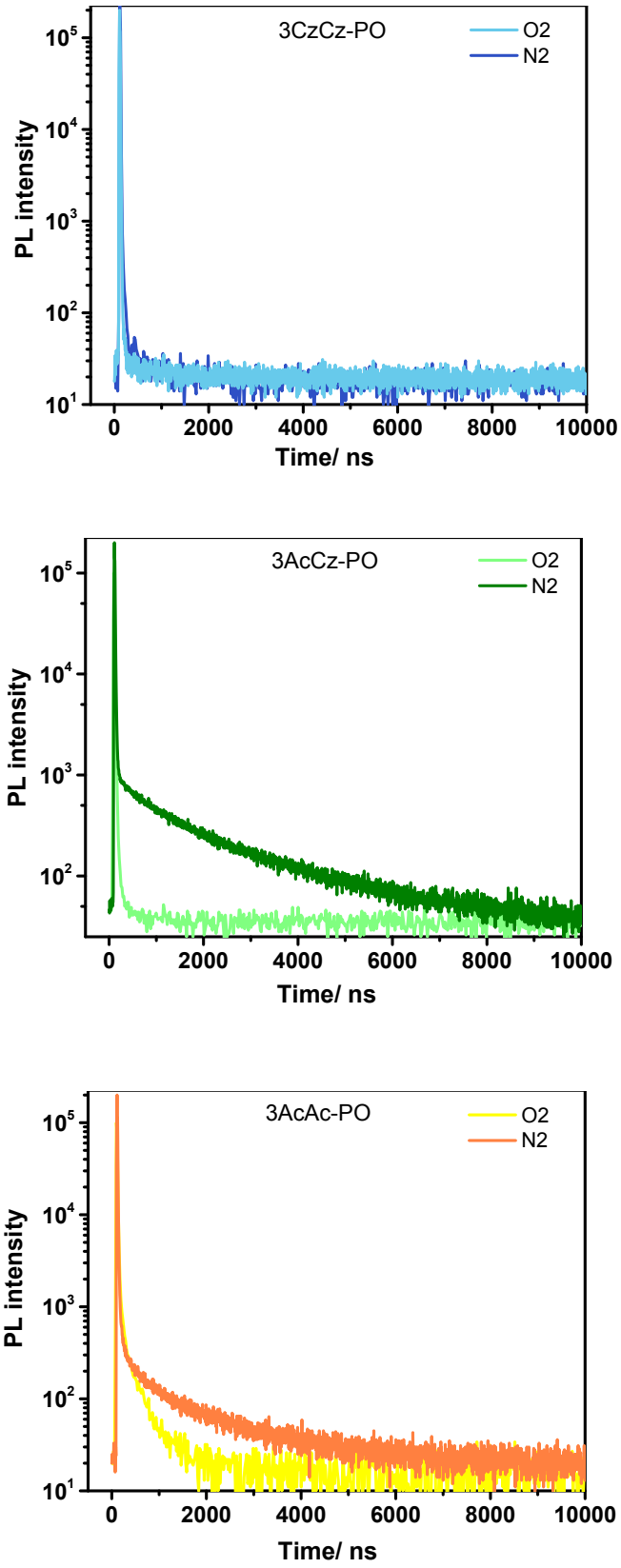

Figure S3. PL decay curves of 3CzCz-PO, 3AcCz-PO and 3AcAc-PO in film under nitrogen and oxygen at 298 K.

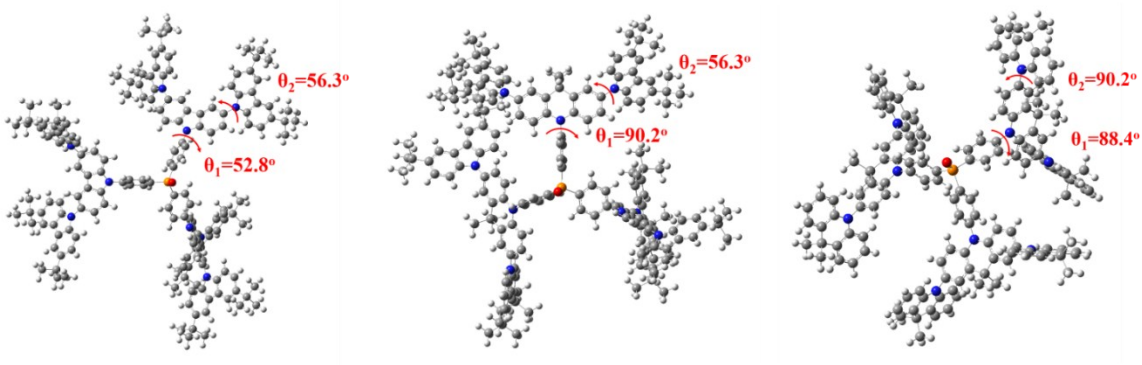

Figure S4. The optimized structure of 3CzCz-PO, 3AcCz-PO and 3AcAc-PO calculated at the B3LYP/6-31G* level by Gaussian 09.

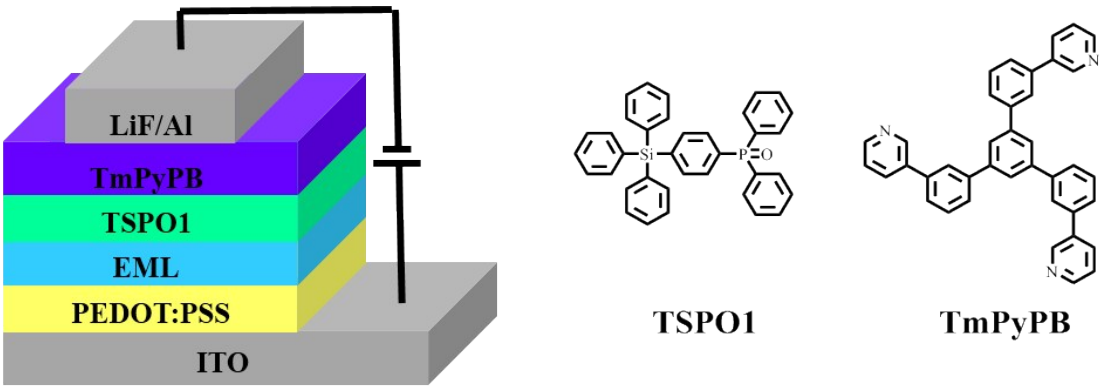

Figure S5. Device structure and corresponding chemical structures

.

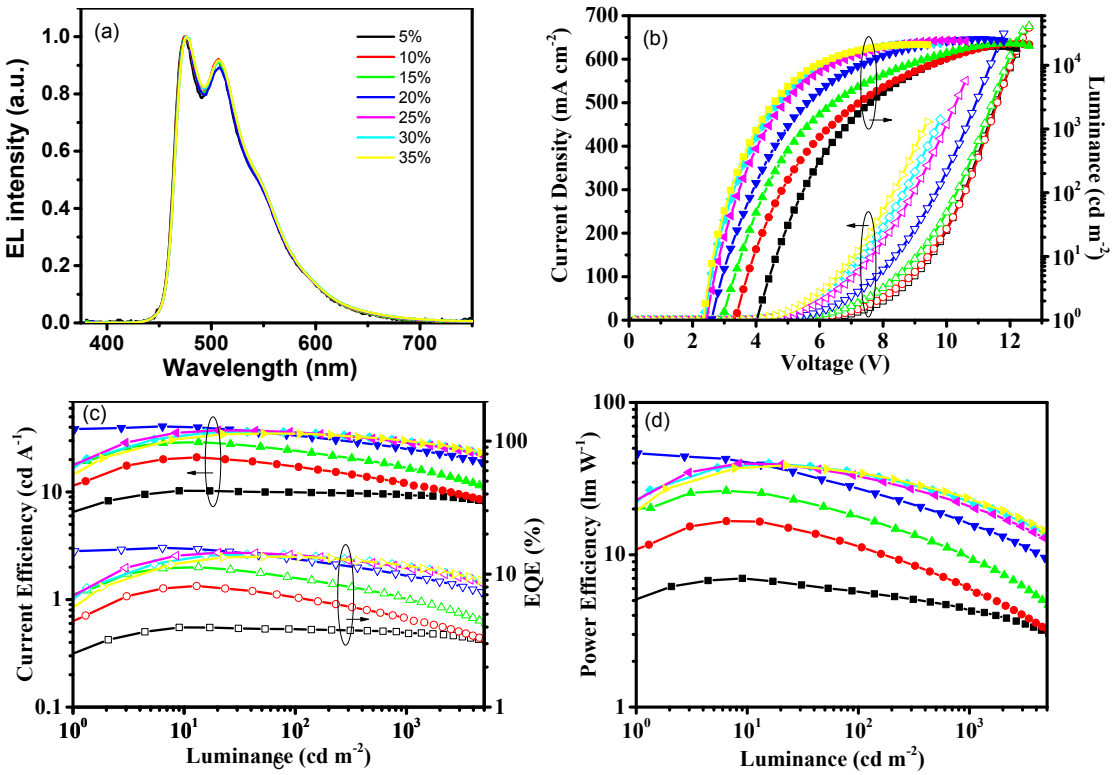

Figure S6. Device performance of 3AcAc-PO as host with different $Ir(mpim)_3$ doping concentration.: (a) EL spectra at a driving voltage of 4 V; (b) current density-voltage-luminance curves; (c) current efficiency and EQE as a function of luminance; (d) power efficiency as a function of luminance.

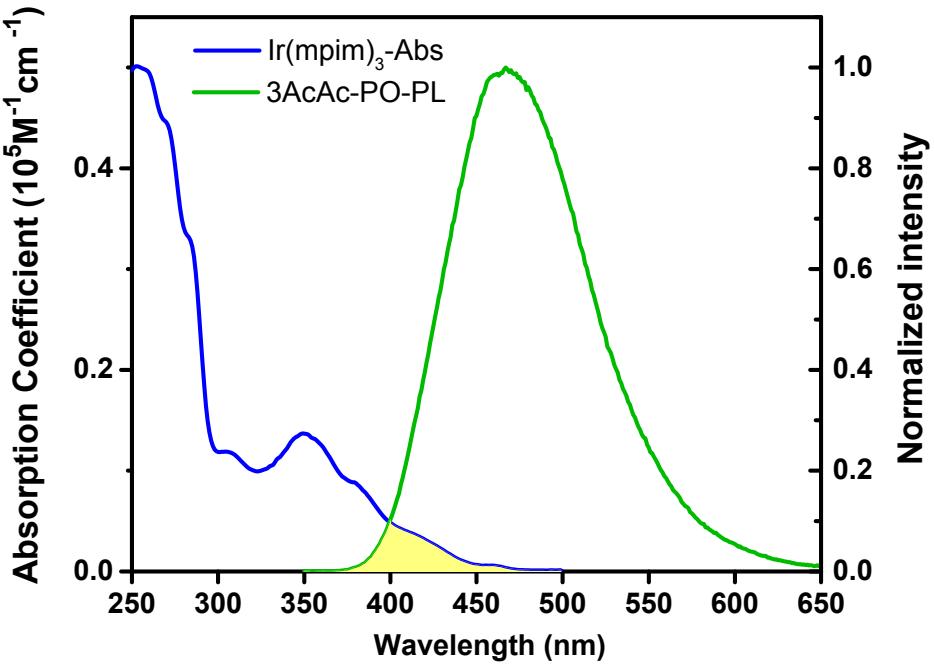

Figure S7. Photoluminescence spectra of 3AcAc-PO in film and absorption of $Ir(mpim)_3$ in CH_2Cl_2 solution (1×10^{-5} mol L^{-1}) at room temperature.

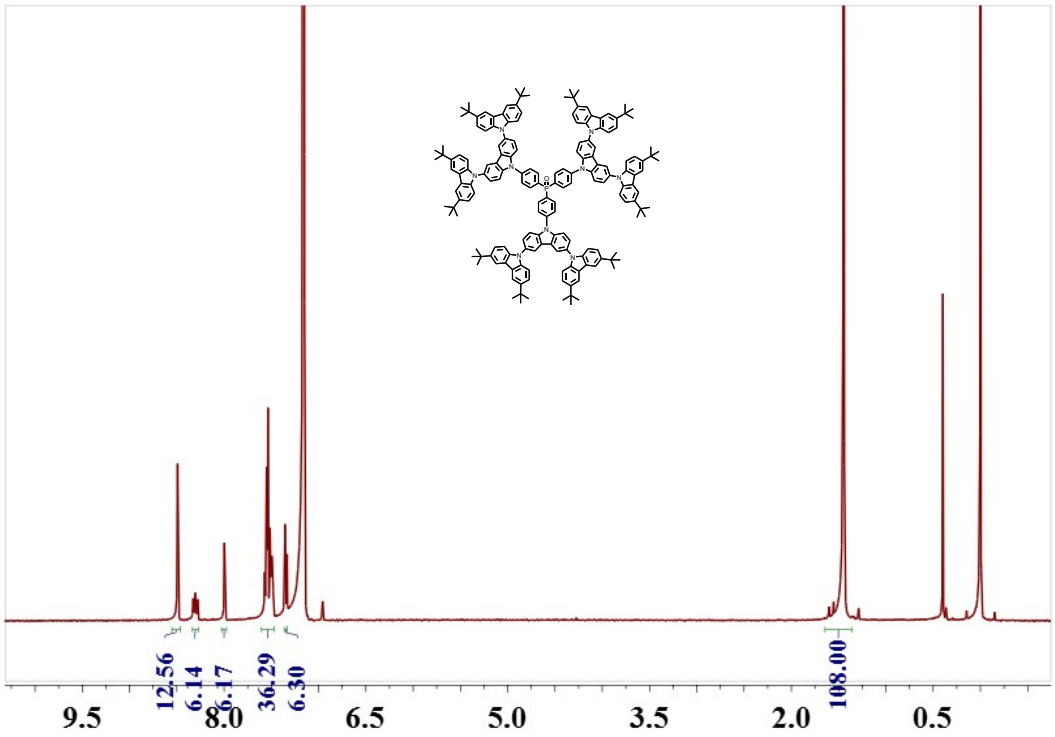

Figure S8. ^{1}H NMR spectrum of **3CzCz-PO**.

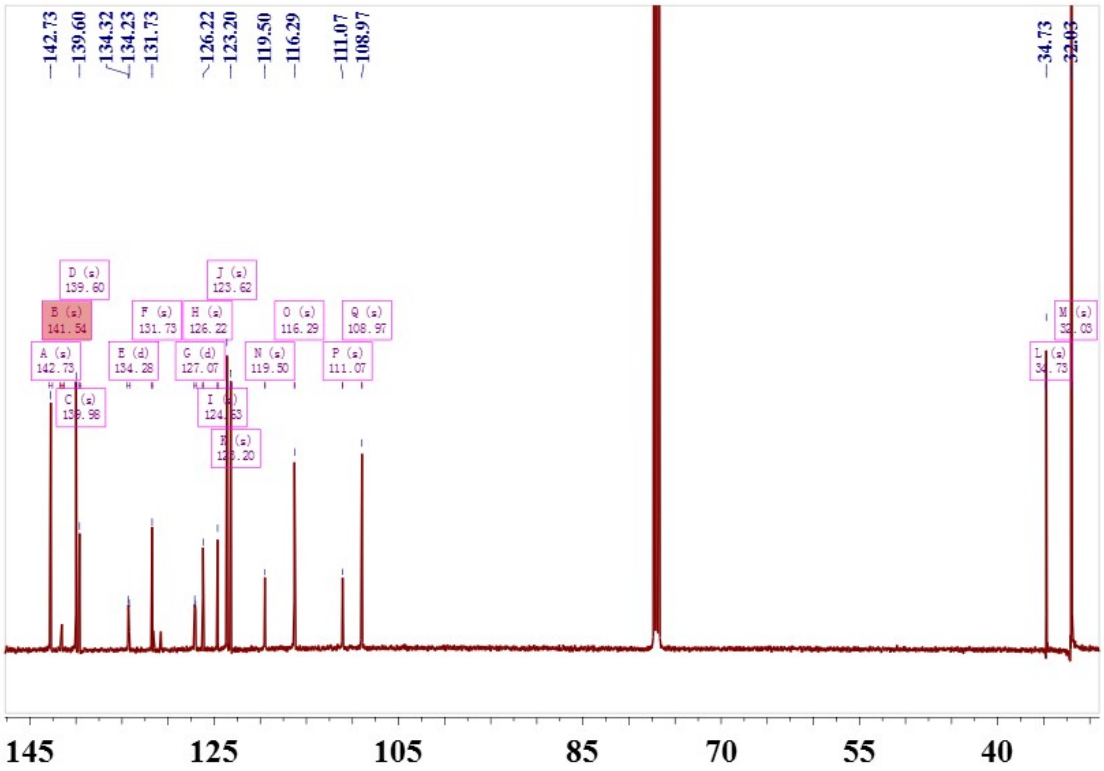

Figure S9. ^{13}C NMR spectrum of **3CzCz-PO**.

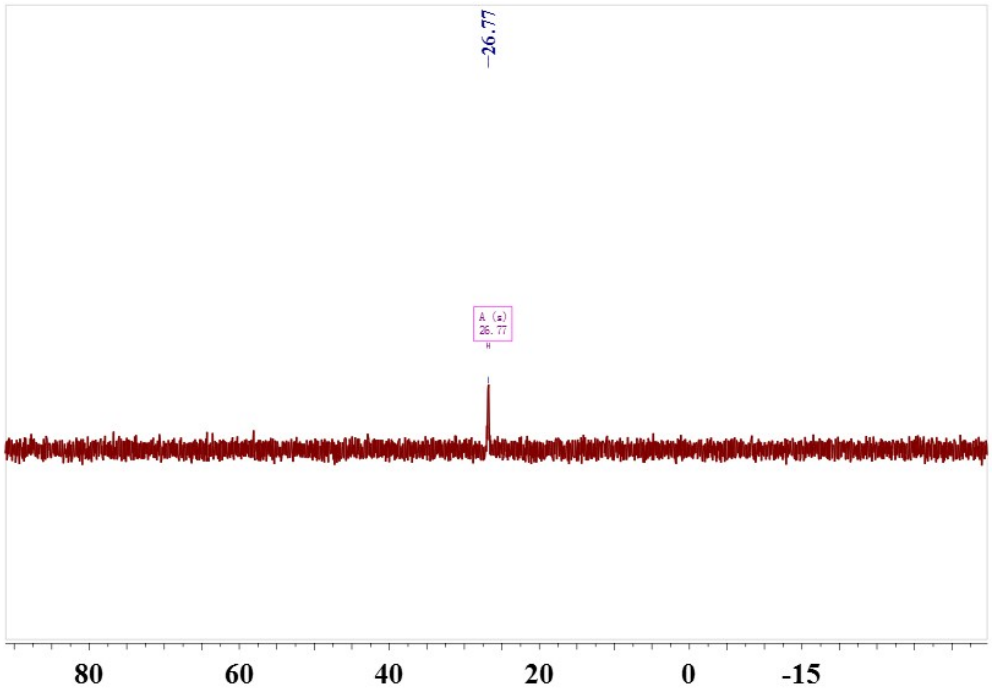

Figure S10. ^{31}P NMR spectrum of **3CzCz-PO**

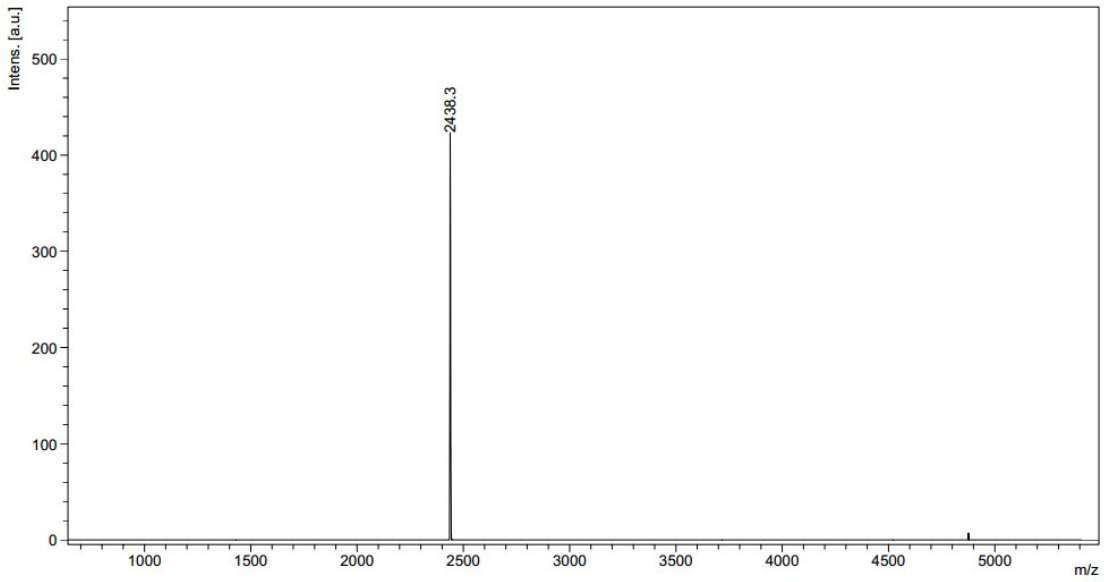

Figure S11. MALDI-TOF spectrum of **3CzCz-PO.**

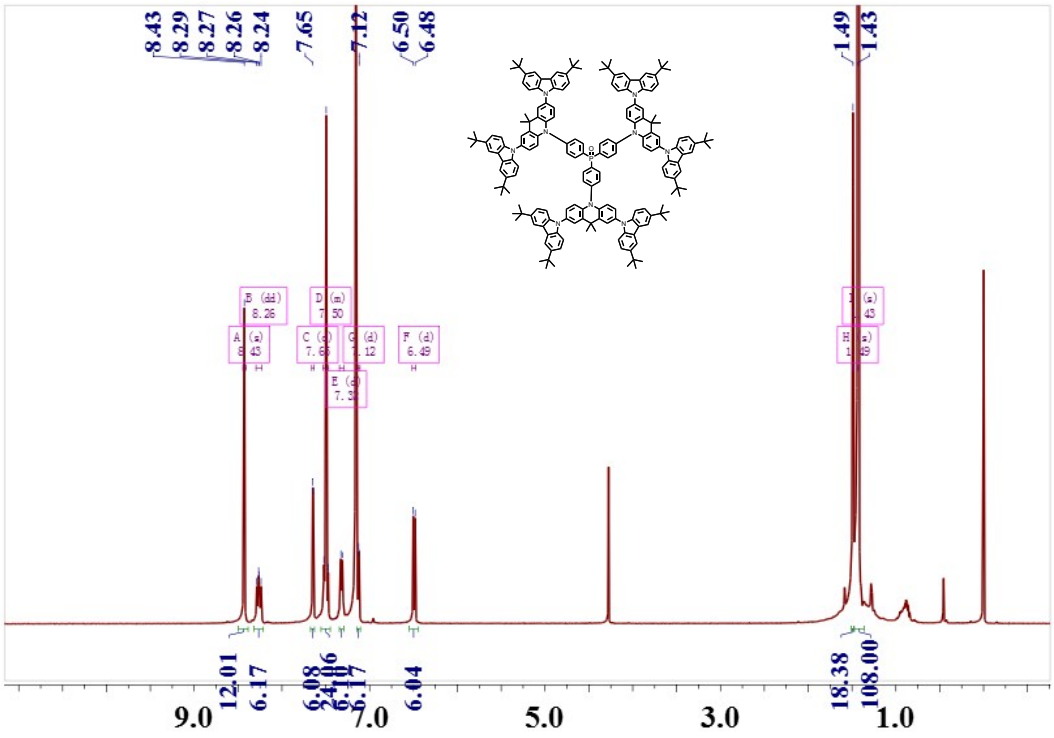

Figure S12. ^{1}H NMR spectrum of **3AcCz-PO**.

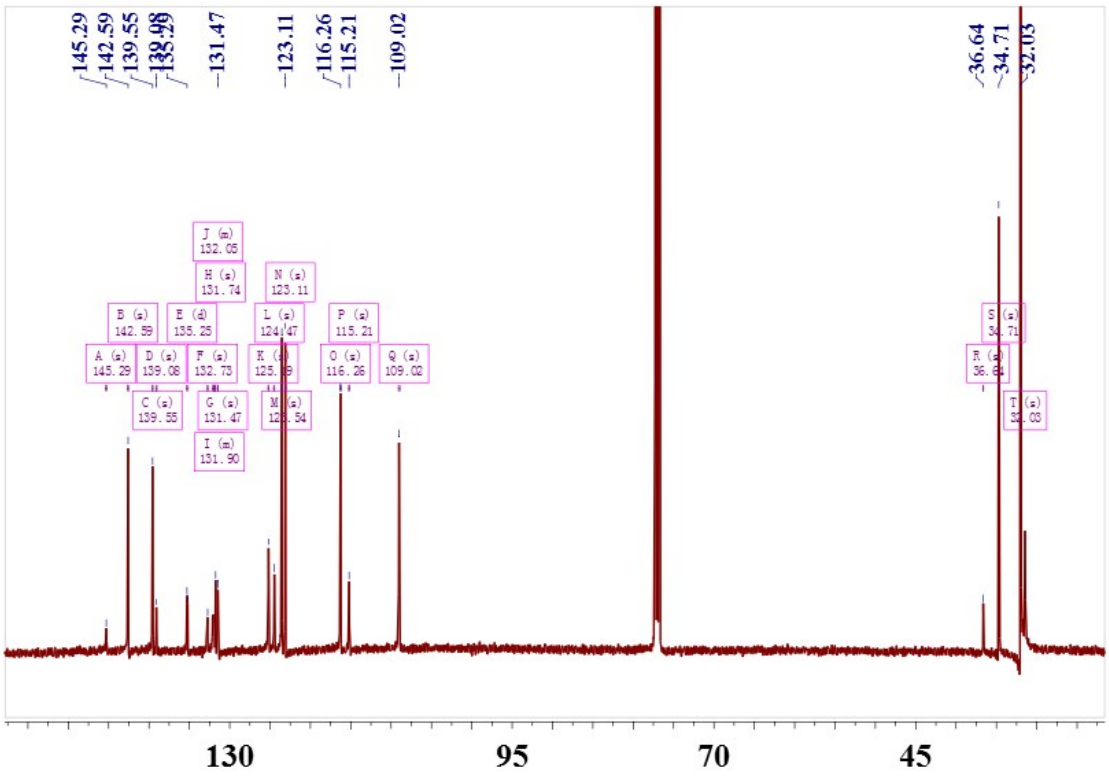

Figure S13. ^{13}C NMR spectrum of **3AcCz-PO**.

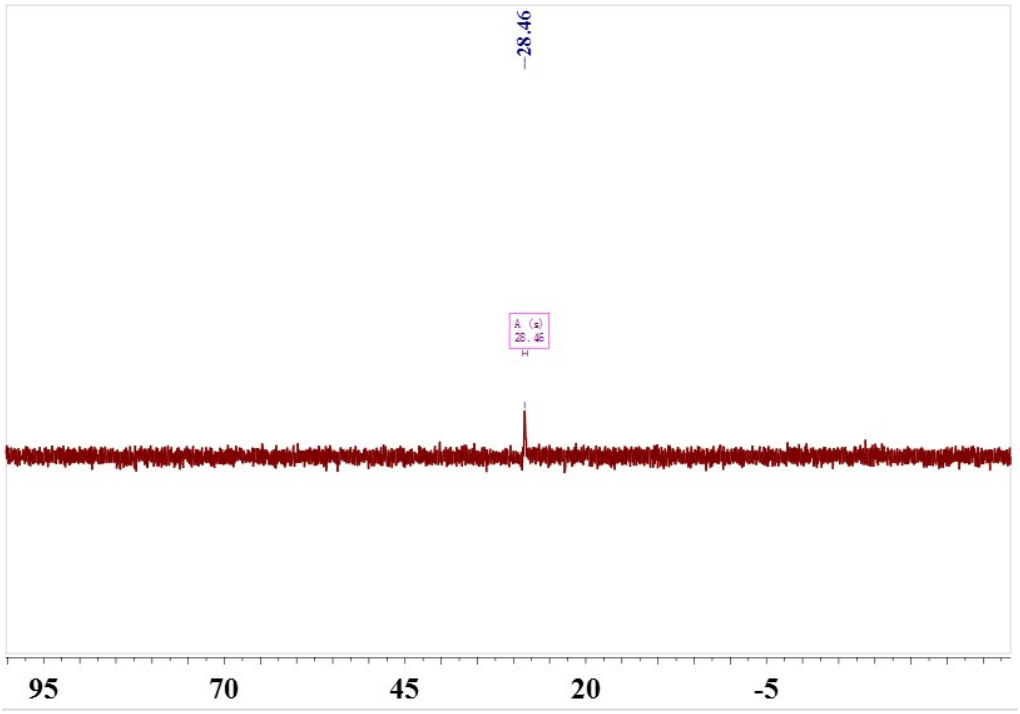

Figure S14. ^{31}P NMR spectrum of **3AcCz-PO**

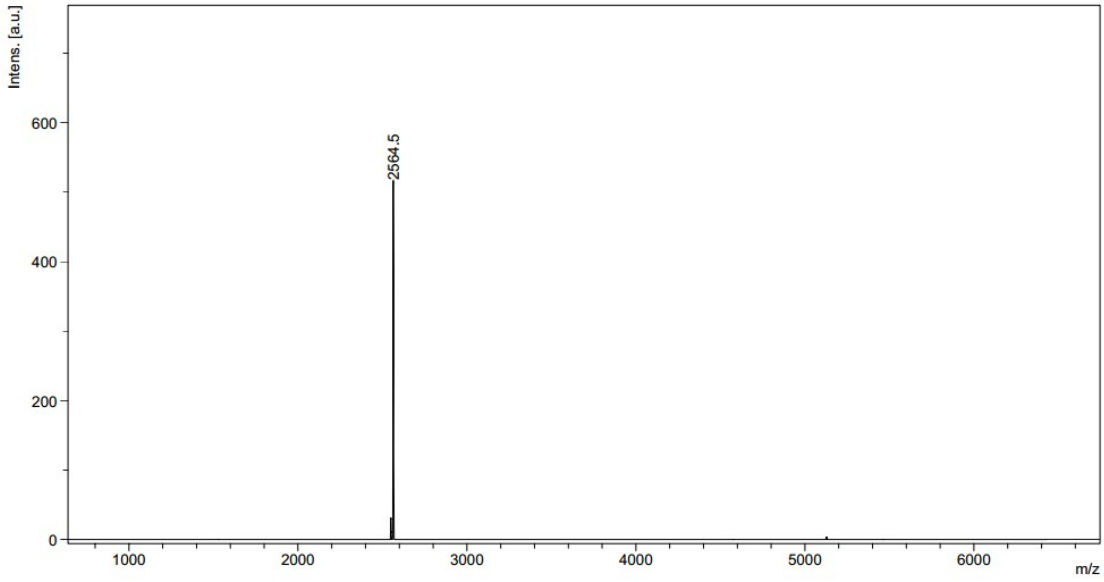

Figure S15. MALDI-TOF spectrum of **3AcCz-PO.**

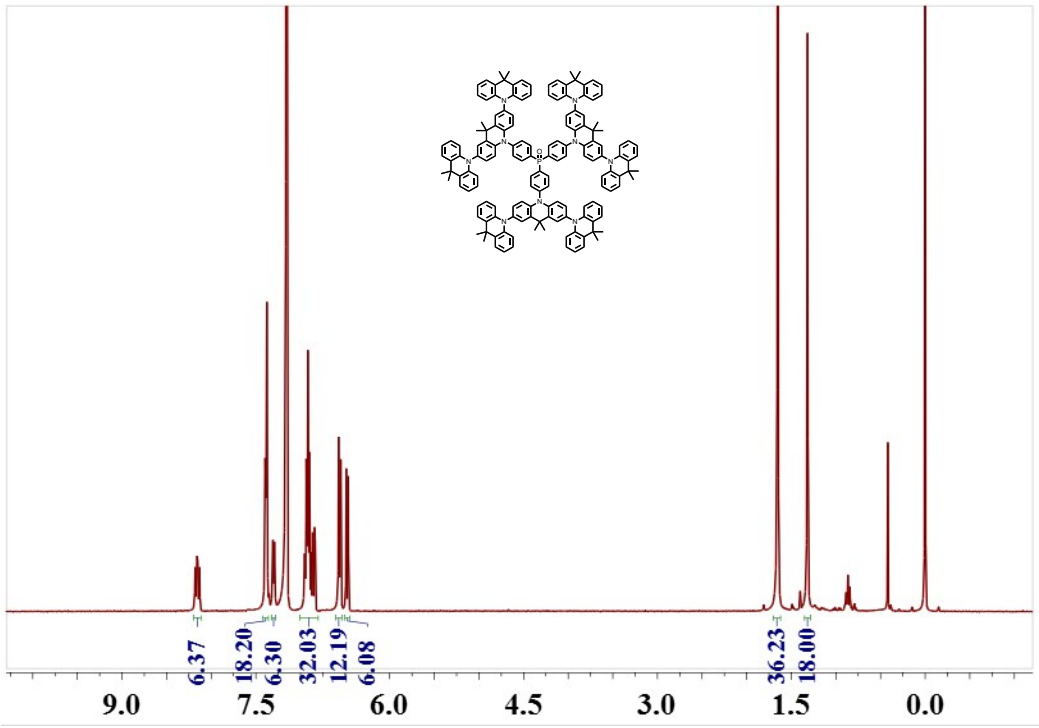

Figure S16. ^{1}H NMR spectrum of **3AcAc-PO**.

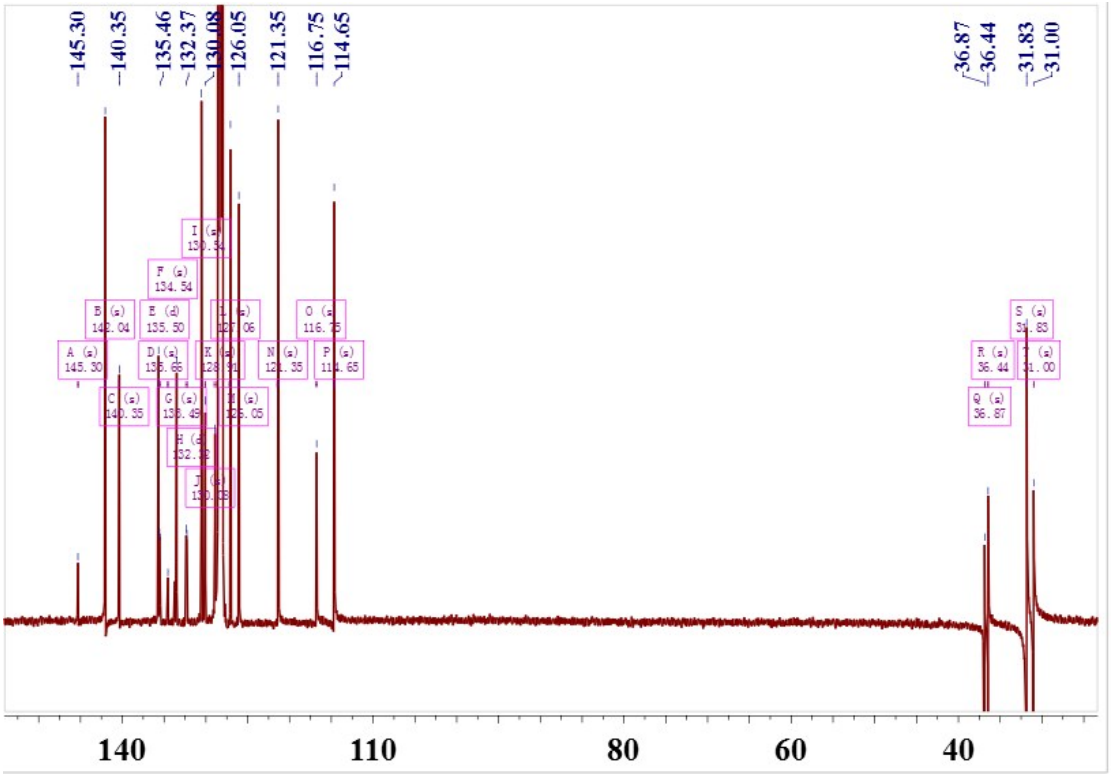

Figure S17. ^{13}C NMR spectrum of **3AcAc-PO**.

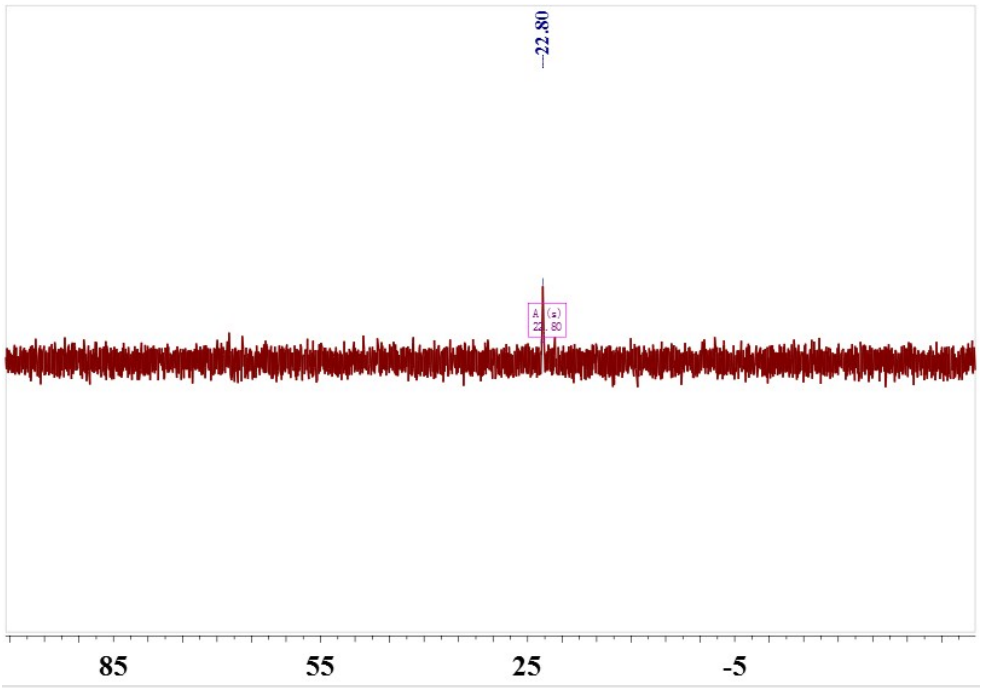

Figure S18. ^{31}P NMR spectrum of **3AcAc-PO.**

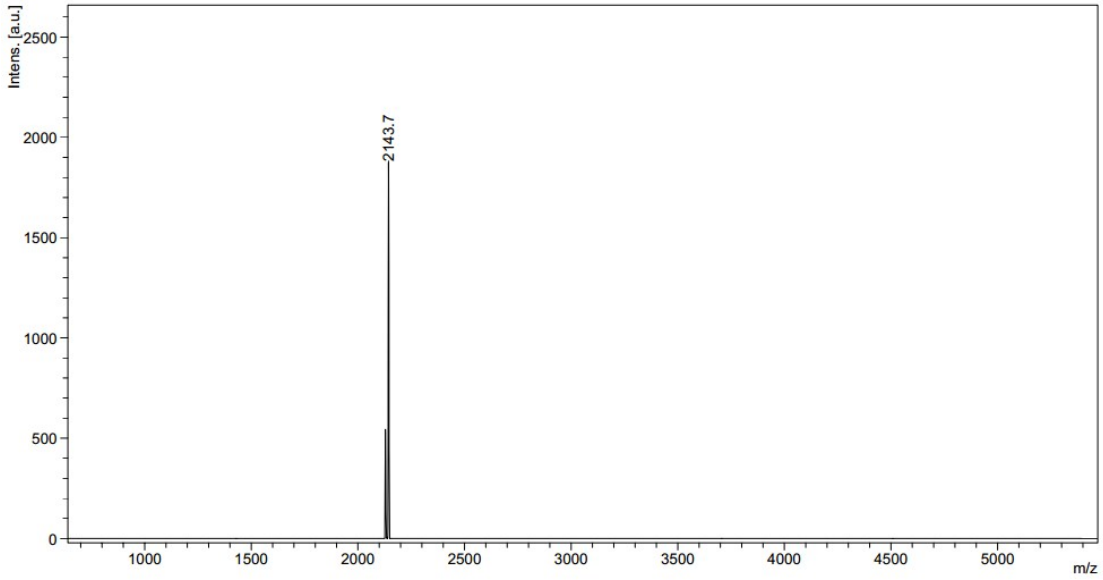

Figure S19. MALDI-TOF spectrum of **3AcAc-PO.**